Spatial Modeling of Rainfall Trends using Satellite Datasets and Geographic Information System

Sanjay Kumar[1*], Deepesh Machiwal[2] and Devi Dayal[2]

[1]Krishi Vigyan Kendra, ICAR-Central Arid Zone Research Institute, Kukma- 370105, Bhuj, Gujarat, India

[2]Regional Research Station, ICAR-Central Arid Zone Research Institute, Kukma- 370105, Bhuj, Gujarat, India

[*]Email of Corresponding Author: dhakadsk@gmail.com

ABSTRACT

This study developed a standard methodology for identifying spatialtrends using satellite-based raster datasets, and demonstrated the methodology for Gujarat State of India where trends in seven rainfall series, i.e. annual, pre-monsoon, monsoon, post-monsoon, non-monsoon, monthly-maximum and one-day maximum, are investigated. It involves the novelty of exploring capabilities of geographic information system in implementing procedures of three trend tests, i.e. Spearman rank order correlation (SROC), Kendall rank correlation (KRC), and Mann-Kendall (MK) tests on raster datasets of Tropical Rainfall Measurement Mission at 0.25°×0.25° resolution. Comparative evaluation of three tests revealed a fair agreement oftestresults in a major portion for pre-, post-, and non-monsoon and one-day maximum rainfall. Whereas, similar results of KRC and MK tests are obtained over considerable area for annual, monsoon and monthly-maximum rainfall. This finding suggested the importance ofselecting appropriatetestdepending on rainfall magnitudes at chosentime scale, andemphasizes robustness of KRC and MK tests. The methodology can be adopted to investigate rainfall trends using satellite-datasets in other parts of the world.

Key words: Rainfall; Satellite dataset; Trend; Statistical test; Geographic Information System

1. INTRODUCTION

Rainfall is one of the key components of the hydrologic cycle that is severely affected from the changing climate globally (Machiwal*et al.* 2016).

Trends in the rainfall series are generally determined by using historical datasets, which are traditionally recordedfrom networks of *in situ*raingauge stations. The rainfall data obtained fromraingaugenetworksare quite expensive especially in arid regions where scantyrainfall is received (Pombo and de Oliveira 2015). On the other hand, there are certain standard rainfall datasets produced by mixing measurements taken from satellite-based sensors and ground observations in order to make the data available for gridded land surface on a regular basis, e.g. the Climate Research Unit (CRU 2000), the Tropical Rainfall Measuring Mission (TRMM) (Huffman *et al.* 1995, 2007), Precipitation Estimation from Remotely Sensed Information using Artificial Neural Networks (PERSIANN) (Sorooshian*et al.* 2000), Climate Prediction Center (CPC) Morphing technique (CMORPH) (Joyce *et al.* 2004), the Global Precipitation Climatology Project (GPCP) (Schneider *et al.* 2010), the National Centers for Environmental Prediction/National Center for Atmospheric Research (NCEP/NCAR) reanalysis dataset (Kanamitsu*et al.* 2002), and the Water and Global Change (WATCH) project (Weedon*et al.* 2011). These satellite-gauge rainfall products are quite popular due to their availability at high spatial resolution (up to grid size of 1°×1°), regular updating, and closeness to the measured raingaugedata (Li *et al.*2014). The only limitation of these datasets is their availability for shorter periods beginning in 1997. In India, several studies examined rainfall trends based on point measurement of rainfall stations (Guhathakurta*et al.* 2011, Sonali and Kumar 2013, Pingale*et al.* 2014, Goyal 2014, Machiwal*et al.* 2016, Sarkar *et al.* 2015, Machiwal and Jha 2016); however, trendstudies dealing with satellite-based datasets are comparatively limited (e.g. Goswami*et al.* 2006, Rajeevan*et al.* 2008, Krishnamurthy *et al.* 2009, Kumar and Jain 2010, Kumar *et al.* 2010, Jain and Kumar 2012, Rathore*et al.* 2013), and theyusually involved the gridded rainfall datasets of 1°×1° spatial resolution. The rainfall data at such spatial scale may not be adequate for understanding local trends for either an entire Indian State (province) or a district.

The nonparametric Mann-Kendall (MK) test is customarily employed for detecting rainfall trends in most studies (Yu *et al.* 2002, Liu *et al.* 2008, Qin *et al.* 2010, Tabari and Talaee 2011, Machiwal*et al.* 2016, Machiwal and Jha 2016). The Kendall's rank correlation (KRC) and MK tests are equally powerful in detecting trends in time series (Machiwal and Jha2008). The nonparametric tests are considered advantageous over the parametric tests as the former are free from assumption of presence of normality that does not remain valid for the most rainfall series (Machiwal and Jha 2016). On the other hand, one of the major assumptions of thenonparametric tests is independence of the datathat is generally not observed as the most rainfall time series exhibit some sort of serial correlation or persistence (Koutsoyiannis and Montanari 2007). Few studies reported that MK test is not robust against presence of serial correlation in time series (e.g. Yue *et al.* 2002), and pre-whitening of the data is required (von Storch 1995). However, another study, i.e. Yue and Wang (2002) extended the works of Yue *et al.* (2002) and emphasized that when trend does exist in a time series, pre-whitening is not

suitable for eliminating the influence of serial correlation on the MK test.Also, recent studies do not advocate pre-whitening approach as it is clearly demonstrated that pre-whitening cannot really improve trend identification when using the MK test, but cause wrong results sometimes (e.g. Sang *et al.* 2014). An alternative to pre-whitening of the data is the modification of trend test to account for the effect of serial correlation (Hamed 2008).

Many past studies have used satellite dataset for detection of trends and variability in rainfall. However, those studies determined trends fora cumulativearea ofcertain pixels, e.g. polygons, zones, regions, etc.by aggregatingrainfall valuesof the pixels falling intothe considered areas (Kumar and Jain 2010, Joshi and Pandey 2011, Oguntunde*et al.* 2011, Das *et al.* 2014, Diem *et al.* 2014, Manzanas*et al.* 2014, Hosciło*et al.* 2015, Bal *et al.* 2016). In most studies, trends in the aggregate rainfall data were detected in a non-spatial manner for the representing areas by treating them as points, and after analysis, the results were passed to geographic information system (GIS) for their spatial presentation (Wagesho*et al.*2013, Westra*et al.*2013, Oza and Kishtawal 2014, Pingale*et al.* 2014, Taxak*et al.* 2014). It is further revealed from the literature that there are relatively less studies where trends are analyzed in a spatially-distributed manner in GIS platform (Gokmen*et al.* 2013, Asadieh and Krakauer 2015). None of such past studies, involving spatially-distributed trend analysis, applied statistical trend tests systematically; preliminary assumption of non-persistence or serial correlation of the datasets was not tested. Therefore, this study proposed, for the first time,a standard methodology for analyzing the spatially-distributed temporal trends in GIS usingsatellite-based rainfalldatasets in a comprehensive manner.

The novelty of the study involves exploring the GIS capabilities in implementing procedure of multipletrend identification tests, i.e. KRC, Spearman rank order correlation (SROC)and MKwith modified MK to remove effect of serial correlation directly on the raster maps of the rainfall distribution with spatial resolution of 0.25°×0.25°. The approach of using multiple statistical tests for trend detectionis highly recommended for the hydrologic parameters (Machiwal and Jha 2008, Sonali and Kumar 2013). The proposed methodology is simple in nature and may havelarge practical utility in analyzing long-term trends usingthe satellite data within a short time frame.The methodologycan also be used to determine distributed-trends in rainfall raster generated from spatial interpolation of point rainfall data. Moreover, the methodology is demonstratedthrough a case study of Gujarat state of India where rainfall trends are detected by applying the suggested procedure.

2.MATERIALS AND METHODS

2.1 Study Area Description

Gujarat state (study area), situated in the western India (Figure 1), is bounded by the Arabian Sea in the western and the southwest directions. Climate of the area is tropical and dry with a great diversity in the climatic conditions over the space. The northwest portion of the area suffers from an extreme climate where the summers are extremely hot while the winters are too cold. During winter season (November-February), the climate remains mild, pleasant and dry

with the mean temperatures ranging from 29°C during day time to 12°C during night. Most parts of Gujarat experience temperature varying from 6 to 45°C (Ray *et al.*2009). During summers (March-May), the area experiences extremely hot and dry climate. Rainfall generally occurs when the southwest monsoon sets on in the area, and accordingly, the entire year can be divided into three seasons, i.e. monsoon (June-September), post-monsoon (October-December) and pre-monsoon (March-May). The mean annual rainfall in the northern and southern portions varies from 510-1020 mm and from 760-1520 mm, respectively. Whereas, the southern highlands of Saurashtra and the Gulf of Cambay experience rainfall of about 630 mm and remaining parts of Saurashtra receive rainfall of less than 630 mm (Kumar *et al.*2014). The driest northwest portion of the area receives the minimum annual rainfall ranging from 250-350 mm (Ray *et al.* 2009).

2.2Rainfall Gridded Data from TRMM

The TRMM datasets consist of products generated for studying precipitation in the tropics. These products include observations of radiances, microwave temperature, radar reflectivity, rainfall rate, vertical rainfall profile, and convective and stratiform heating. TRMM was launched on November 27, 1997 and decommissioned on April 15, 2015. It re-entered Earth's atmosphere in June 2015 (GSFC 2015)**.** Because the total days in each month are different, mm/hr is used for easy comparison between the months. Both daily and the hourly averages of monthly data (3B42; Version-7) were downloaded from the TRMM website (TRMM, 2015). All the data (January 1998 to October 2014) were downloaded in Network Common Data Form (NetCDF) of 0.25°×0.25° resolutions. The NetCDF is a set of software libraries and self describing, machine-independent data formats that support the creation, access and array oriented scientific data. This NetCDF data was imported as raster layer using Make NetCDF Raster Layer tool in GIS software. Since the 3B43 product is an hourly average of the particular month, it has been converted in to monthly rainfall by multiplying the hourly rain rate with the total hours in that month. Total 6148 layers of daily data and 202 layers of monthly data were imported in GIS for preparing annual, monsoon (June-September), pre-monsoon (March-May), post-monsoon (October-December), Non-monsoon (excluding monsoon), one-day maximum and monthly maximum raster layers. Apart from TRMM data, SRTM Digital Elevation Model (DEM) was also used to derive information about physiography of the area.

The variability in annual rainfall was assessed by computingthe mean, standard deviation (SD) and coefficient of variation (CV). These statistics were developed spatially using annual rainfall (1998-2013) in raster format and district-wise means were also estimated.

2.3Developing GIS-Based Methodology for Identifying Spatial Trends using Raster Datasets

To the authors' knowledge, until now there has been no study explicitly describing a methodology for the analysis of spatial trends in GIS environment. Hence, in this study, a GIS-based methodology is developed to apply statistical trend tests on raster datasets using appropriate GIS tools. Three non-parametric statistical tests, i.e. SROC, KRC, and MK tests are selected for analyzing the spatial trends in gridded rainfall data. This study utilized the useful geo-processing tools by combining them in the model builder module of ArcMap software in order to optimize the number of steps required to be performed for applying the tests. The developed methodology explains a proper sequence of the tools and adequate flow of different operations for detecting trends in spatial datasets using the GIS capabilities. This methodology may also help in customization of different tools to develop single tool for analyzing trends on raster datasets of high resolutions. The presented methodology may be easily adopted for analyzing presence/absence of the trends in other datasets over the globe. The detailed procedure for applying the tests using the developed methodology is illustrated below.

2.3.1 Spearman Rank Order Correlation Test

The SROC is a nonparametric test, which is usually used to check the existence of long-term trends (McGhee 1985, WMO 1988). The step-by-step procedure for applying this test in the GIS platform using raster datasets is described below.

(i) Arrange n number of raster datasets (x_t) sequentially year wise starting from first year (t = 1) to the last year (t = n).

(ii) Use 'rank tool' to generate n number of 'rank raster' datasets (Give rank in decreasing order while running the tool in batch mode) where first raster map contains the largest value of the rainfall amounts for every cell (or pixel), and the last raster map retains the smallest value for every cell.

(iii) Compare first year raster map of the original dataset with the every map of n 'rank raster' datasets one-by-one by using 'equal to tool'. If the values of two raster maps are equal for a cell then assign 1 to that cell; otherwise zero. This process will generate n number of [1,0] raster datasets with value of 1 for a cell in i^{th} number of raster indicating the i^{th} rank of the rainfall amount of that cell in the first year.

(iv) Use 'iterate tool' for picking all original raster datasets one by one prior to repeat the last step for comparing the next 'rank raster' dataset with the every original raster datasets. This will generate another n number of [1,0] raster datasets where 1 will simply indicate ranks of rainfall amounts occurred in the second year for a given cell. Similarly, use the iterative tool n times to compare n original raster datasets one-by-one with all n 'rank raster' datasets, and generate $n \times n$ [1,0] raster datasets.

(v) Multiply 1st [1,0] raster map (where 1 indicates presence of the largest rainfall values in first year) of first n datasets with 1 by using 'times tool'. Similarly, multiply 2nd [1,0] raster

map (indicating presence of the second-largest values in first year) with 2, and then repeat this process up to the last or n^{th} [1,0] raster map (indicating the presence of the smallest values in the first year) of first dataset by multiplying with n. Repeat this multiplication process for the second n datasets by multiplying them from 1 to n sequentially in batch mode, and so on for all n datasets. Finally, there will be $n \times n$ number of raster datasets with first n datasets [{1,0}, {2,0}, …, {n,0}] representing only the ranks of the first year rainfall data within spatial time series of size n, and so on.

(vi) Add n raster datasets [{1,0}, {2,0}, …, {n,0}] sequentially by using 'cell statistics tool' to generate n number of R_{xt} raster dataset with $R_{xt} = 1$ for the largest x_t and $R_{xt} = n$ for the smallest x_t. Hence, the R_{xt}raster datasets basically replace the original rainfall values in successive years with their respective ranks over the n period of years.

(vii) The R_{xt}raster dataset were used to compute other raster datasets d_t ($d_t = R_{xt} - t$) for n = 1, 2, …n by using 'minus tool' in batch mode. The raster dataset d_t was used to calculate r_s raster dataset as shown by the following expression (Machiwal and Jha 2012):

$$r_s = 1 - \frac{6\sum_{t=1}^{n} {d_t}^2}{n(n^2-1)} \quad (1)$$

(viii) The $r_s$rasters were utilized to compute the test-statistics given in the following equation (Machiwal and Jha 2012):

$$t_s = r_s\sqrt{\frac{n-2}{1-{r_s}^2}} \quad (2)$$

The step-by-step procedure for performing this test in GIS platform by using raster datasets is explained by a flowchart as shown in Figure 2. The significance of the presence/absence of the trends was checked by comparing the computed t_s raster with the critical values at three level of significance (l.s.), i.e. 0.01, 0.05 and 0.10. The critical values were taken from the t distribution for the chosen l.s. of α and n-2 degrees of freedom. The critical values (n = 17) were taken as 2.602, 1.753 and 1.34 at 0.01, 0.05 and 0.10 l.s., respectively.

2.3.2 Kendall's Rank Correlation Test

The KRC is one of the most preferred tests for trend detection in hydrologic time series (Jayawardena and Lai 1989**,** Kumar 2003). The steps describing procedure for applying this test are elaborated below.

(i) In sequentially-arranged raster rainfall datasets x_t (t = 1, 2, …,n) of n years, compare first year raster x_1 with all the subsequent years' rasters (x_2, x_3, …, x_n) one-by-one. This may be done by taking difference of two rasters, x_i-x_j (j>i) in all pairs of raster dataset using 'minus tool', and generating [+,-] raster datasets depending upon the relative values of the two

rastersx_i and x_j. Repeat this process by comparing second year raster x_2 with all the subsequent rasters ($x_3, x_4, \ldots, x_n$) one-by-one, and so on up to comparing $x_{n-1}$with x_n raster.

(ii) Use 'reclassify tool' to classify the [+,-] raster datasets into two classes, i.e. 1 (positive values) and 0 (negative values). This step will convert [+,-] raster datasets into [1,0] raster datasets.

(iii) Use 'cell statistics tool' for adding all the [1,0] rasters, and name the resultant raster dataset as *P*, which defines the number of times the condition of $x_j > x_i$ is satisfied among all pairs of raster datasets.

(iv) Compute τ raster and variance of τ, $\{Var(\tau)\}$ based on the *P* raster dataset and value of *n* using the following expressions (Kendall 1973, Machiwal and Jha 2012):

$$\tau = \frac{4P}{n(n-1)} - 1 \quad (3)$$

$$\text{and, } Var(\tau) = \frac{2(2n+5)}{9n(n-1)} \quad (4)$$

(v) Finally, calculate the observed test-statistics (z) by using the equation as follows:

$$z = \frac{\tau}{\sqrt{Var(\tau)}} \quad (5)$$

A flowchart depicting the procedure for performing this test in GIS platform on raster datasets is explained in Figure 2. The observed values of the *z*-statistics were compared their critical limits of $\pm$2.58, $\pm$1.96 and $\pm$1.64 at l.s. of 0.01, 0.05 and 0.10, respectively. If the observed value of the *z*-statistic lies within these limits, the null hypothesis of no trend cannot be rejected.

2.3.3 Mann-Kendall Test

The MK test is customary and widely-used nonparametric test that explores the trend in a time series with indicating type of trend (i.e. increasing or decreasing). Detailed procedure for implementing this test in GIS for identifying trends in raster datasets is explained in few steps as follows:

(i) Follow first step of the KRC test to generate [+,-] raster datasets using 'minus tool'.

(ii) Classify the [+,-] raster datasets into three classes, i.e. 1 (negative values), -1 (positive values), and 0 (zero values) using 'reclassify tool'. This step will convert [+,-] raster datasets into [-1,0,1] raster datasets.

(iii) Add all the [-1,0,1] rasters by using 'cell statistics tool', and name the resultant raster dataset as *S* raster.

(iv) Identify tied values (e_i) and their groups (g) as indicated by 0 cells in [-1,0,1] rasters. Add all the tied values in each group by using 'cell statistics tool' and generate e_i raster for every group.

(v) Generate another m raster [1,-1] from S raster by using 'reclassify tool' with the conditions to classify any cell value as 1 for the value of S less than zero, and as -1 for the value of S greater than zero.

(vi) Combine both S and $m$rasters to compute the test-statistic raster (U_c) as defined in the following expression (Machiwal and Jha 2012):

$$U_c = \frac{S+m}{\sqrt{V(s)}} \tag{6}$$

$$\text{where,} \quad V(s) = \frac{1}{18}\left[n(n-1)(2n+5) - \sum_{i=1}^{g} e_i(e_i-1)(2e_i+5)\right] \tag{7}$$

The observed values of U_c-statistic were compared with the critical limits of $\pm$2.58, $\pm$1.96 and $\pm$1.64 at l.s. of 0.01, 0.05 and 0.10, respectively. The flowchart explaining the entire procedure for applying the test in the GIS framework is illustrated in Figure 2.

2.3.4 Modified MK Test for Removing Effect of Serial Correlation

In this study, the effect of serial correlation on the MK test was removed by adopting the approach of effective sample size as proposed by Lettenmaier(1976). The presence of serial correlation was examined by performing autocorrelation analysis for all seven types of rainfall rasters, i.e. annual, seasonal (pre-monsoon, monsoon, post-monsoon, non-monsoon) and extremes (one-day maximum and monthly maximum) rainfall series. The serial correlation (r_k) in the raster dataset was examinedby estimating autocorrelation coefficient/function (r_k) using the following expression (Machiwal and Jha 2012):

$$r_k = \frac{\sum_{t=0}^{n-k} x_t x_{t+k} - \left(\frac{1}{n-k}\right)\sum_{t=0}^{n-k} x_t \sum_{t=0}^{n-k} x_{t+k}}{\sqrt{\left[\sum_{t=0}^{n-k} x_t{}^2 - \left(\frac{1}{n-k}\right)\left(\sum_{t=0}^{n-k} x_t\right)^2\right]}\sqrt{\left[\sum_{t=0}^{n-k} x_{t+k}{}^2 - \left(\frac{1}{n-k}\right)\left(\sum_{t=0}^{n-k} x_{t+k}\right)^2\right]}} \tag{8}$$

The steps to compute$r_k$at lag-1 using raster datasets, shown in the flowchart (Figure 2), are explained below.

(i) In sequentially-arranged raster rainfall datasets x_t (t = *1, 2, ...,n*) of n years, use 'Square tool' in batch mode over x_t (t = *1, 2, ..., n*) for getting $n$squaredrasters.

(ii) Compute $x_t x_{t+1}$ (t = 1, 2, …,*n-1*)rasters using 'Times tool' in batch mode; the output will be *(n-1)*rasters.

(iii) Use 'Cell Statistics tool' for computing$\sum x_t$ (t = *1, 2, ...,n-1*), $\sum x_{t+1}$ (t = *2, ...,n*), $\sum x_t{}^2$(t = 1, 2, …, *n-1*), $\sum x_{t+1}{}^2$(t = *2, ..., n*) and $\sum x_t x_{t+1}$(t = 1, 2, …, *n-1*) in batch mode.

After computing the above-defined five input rasters,use model builder to formulate eq. (8)and develop new toolfor completingentire process in one click and the same tool is applied on all other time series after defining input parameters.

The null hypothesis (H_o) of no serial correlation was then tested by comparing the value of lag-1 autocorrelation coefficientfrom the upper and lower critical limits calculated using thefollowing equations (Machiwal and Jha 2012).

$$(r_k)_{upper} = \left[\frac{1}{(n-k)}\right]\left[-1 + z_{1-\propto/2}\sqrt{(n-k-1)}\right] \quad (9)$$

$$(r_k)_{lower} = \left[\frac{1}{(n-k)}\right]\left[-1 - z_{1-\propto/2}\sqrt{(n-k-1)}\right] \quad (10)$$

where, $z_{1-\alpha/2}$=standard normal variate at l.s. of α. If $(r_k)_{upper}<r_k<(r_k)_{lower}$, the $H_o$ofr_k =0isrejectedandthisindicatesthattherainfallseriesis notpurelyrandomandsomeserial correlation or persistenceexists; otherwise,the H_o cannot be rejected (Machiwal and Jha 2012). The values of $z_{1-\alpha/2}$are 1.645, 1.965 and 2.326 at 0.10, 0.05 and 0.01 l.s., respectively (Pingale*et al.* 2014).In this study, presence of the serial correlation was examined at 0.01 and 0.05 l.s.

In the rasters, containing values of the original MK test-statistics, i.e. *Uc*, were then replaced with the modified test-statistic valuesfor the pixels where serial correlation was found to be present.The mathematical expressionproposed by Lettenmaier (1976)tocalculate modified MK test-statisticvalue (z^*)is as follows:

$$z^* = U_c(\sqrt{n^*/n}) \quad (11)$$

where, n^*/n is termed as the correction factor computed for the autocorrelation function (r_1) at lag-1 autoregressive process from the following expression (Matalas and Langbein, 1962):

$$n^*/n = \frac{1}{1+2\frac{r_1{}^{n+1}-nr_1{}^2+(n-1)r_1}{n(r_1-1)^2}} \quad (12)$$

Following the above procedure, the effect of serial correlationfrom the MK test results was removed from all the rainfall data series.

2.4Application of the Developed Methodology

The developed GIS-based methodology of three trend detection tests is demonstrated by applying it to identify the trends over the Gujarat State of India using TRMM rainfall datasets. The trendsare detected in seven rainfall variable, i.e. annual, pre-monsoon, monsoon, post-monsoon, non-monsoon, one-day maximum, and monthly maximum rainfall using spatial dataset for a period of16-year and 10 months (January 1998-October 2014).Analyses of this study based on about 17-year period TRMM datasetsmay not representative of long-term

rainfall trendsin the study area, and hence, the relative significance of the results may be enhanced by including more years' data with theirincreased availability in future.

2.5 Comparative Evaluation of Trend Tests

Results of the three trend tests are spatially-compared through overlay analysis in GIS platform where, spatial variability of the rainfall trends under three l.s. of 0.01, 0.05, and 0.10 is explored, and areas having increasing/decreasing rainfall trends are delineated by considering the similar results obtained from at least two tests. The results of the three tests are compared over the space by performing union analysis based on five combinations of the similar/dissimilar results, i.e. similar results of minimum of two tests (SROC-KRC, SROC-MK, KRC-MK, and SROC-KRC-MK), and dissimilar results of all the tests.

3. RESULTS AND DISCUSSION

3.1 Spatial Statistics of Mean Annual Rainfall

The spatial statistics, i.e. mean,SD and CV, of the annual rainfall are presented in Figure 3. It is seen from Figure 3a that the annual rainfall is the lowest (400-700 mm) in the northwest portion covered by the Kachchh district, whereas it is the highest (>1500 mm) in Valsad district located in the southern portion. In Gujarat, 10 of the total 26 districts showed the mean annual rainfall of more than 1000 mm (Table 1). This indicates large spatial variations of the mean annual rainfall over the study areain comparison to previous studies reported for Gujarat (Ray *et al.* 2009; Kumar *et al.* 2010). It is further seen that the SD of the annual rainfall varied from less than 200 mm (northern portion) to more than 350 mm (middle portion). However, in a major portion (74643.9 km^2) of the area, located in southwest and southern part, the SD of the annual rainfall ranges from 300-350 mm (Figure 3b). The lowest value of the SD is obtained as 229 mm for Kachchh district and the highest as 415 mm for Anand district.The variability of CV of the annual rainfall ranges from less than 20% to more than 50% (Figure 3c). The CV of the annual rainfall is very high (> 40%) for seven districts, i.e. Rajkot, Ahmedabad, Anand, Surendranagar, Patan, Jamnagar and Kachchh (Table 1). The CV values are more than 50% in the northernKachchh district, which are in close agreement with Machiwal et al. (2016). On the other hand, three districts situated at the southern end (Figure 3c) showed the CV of less than 20% with itslowest value (17%) for Dang district. Kumar *et al.* (2010)reported the average CV of annual rainfall for Gujarat as 31%. It is clearly revealed from the above discussion that the SD and CV are the highest in the northern and northwest portions of the area indicating large spatial variations where the mean annual rainfall is very low.

3.2 Presence of Serial Correlation

The serial correlation in all seven rainfall series was examined at lag-1 and results are presented in Figure 4. It is revealed that serial correlation is present over large areas in all the rainfall series ranging from 18878.3 km^2(10.2%)for one-day maximum rainfall to 60961.1 km^2

(32.8%) in southwest portion for monthly-maximum rainfall (Figure 4f,g).In case of annual rainfall, the serial correlation ismostly found in middle-northern districts, i.e. Patan, Banaskantha, Sabarkantha, Gandhinagar, Ahmedabad, Bhavnagar, Bharuch, Anand, Kheda, Panch Mahal, Dahod and Vadodara (Figure 4a).In pre-monsoon and monsoon rainfall, the serial correlation was significant over 20525 km^2(11%)and 57354.1 km^2(30.8%) areas, respectively (Figure 4b,c).In post-monsoon rainfall, the serial correlationwas dominatingin 46251.6 km^2(24.9%) overKachchh and adjoining parts (Figure 4d). In non-monsoon rainfall,serial correlationwas prominent in 25703.7 km^2(13.8%) in eastern Kachchh, western Patan and parts of Surendranagar, Rajkot, Kheda, PanchMahal, Vadodara and Navsari districts (Figure 4e).

3.3 Spatial Distribution of Rainfall Trends

3.3.1 Annual Rainfall

Spatially-distributed trends ofthe annual rainfall identified by three tests areillustrated in Figure 5. Results of the SROC test (Figure 5a) showed that the annual rainfall is having significant trends at 0.10 l.s. over 146101.7 km^2 (78.6%) spreading all over the area except in the southern portion and some pockets in middle, southwest and northwest regions (Figure 5a). Similarly, the trends are found statistically-significant at 0.05 l.s. in 85145.5 km^2 (45.8% area) located in ten districts, i.e. Kachchh, Banaskantha, Sabarkantha, Jamnagar, Rajkot, Surendranagar, Amreli, Patan, Panchmahal and Dahod. The highly-significant trendsat 0.01 l.saredistributed over pockets of Kachchh, Banaskantha, Sabarkantha, Jamnagar, Rajkot districts covering 5745.6 km^2 (3.1%) area. Of the total 26 districts, only 8 were found having the non-significant trends (Table 2).

Results of the KRC test shown in Figure 5b indicated that the annual rainfall has increasing trends in 173745.9 km^2 (93.5% area) and decreasing trends in 12165.5 km^2 (6.5% area). However, the increasing trends are found statistically-significant in 84544.1 (45.5%), 32857.3 (17.7%) and 309.1 (0.2%) km^2 at 0.10, 0.05 and 0.01 l.s., respectively. The significantly increasing trends at 0.05 l.s. are visible in the northwest and southwest portions where Saurashtra-Kachchh region exists and in the northeast portion (Figure 5b) comprising of six districts, i.e. Kachchh, Amreli, Banaskantha, Sabarkantha, Jamnagar, and Panchmahal. Similarly, significantly-increasing rainfall trends are reported by Machiwal et al. (2016) for the northenKachchh district of Gujarat. Furthermore, the decreasing trends are seen only in the southern portion covering entire Valsad and The Dangs districts, and parts of Navsari, Tapi, Surat and Narmada districts. However, none of the decreasing trends are found significant at any l.s. It is seen from Table 3 that the results of the KRC test revealed a significant increase in the annual rainfall for ten districts at 0.10 l.s.

It can be seen from Figure 5cthat the increasing MK trends are present in 176086.6 km^2 (94.7%) all over the area except in the southern portion where decreasing trends are present in

9824.8 km^2 (5.3%). However, Kumar *et al.*(2010) reported the increasing trends in June and August months and decreasing trends in July and Septembermonths.The increasing trends are statistically-significant at 0.10 l.s. in 74124.6 km^2 (39.9%) area, mostly situated in the Saurashtra-Kachchh region and in a fringe located in the northeast portion. This finding matches well with that reported by Machiwal et al. (2016) for Kachchh district. The highly-significant increasing trendsat 0.05 l.s. are found in 18200.1 km^2 (9.8%) area. The MK test couldnot detect significant trendsat 0.01 l.s. The significantly increasing rainfall is detected in 6 districts of the area at l.s. of 0.10 (Table 4).

It is clear from the above discussion that the results of three tests agree, in general, with each other. However, there is close agreement within the results of the KRC and MK tests. The SROC test does not tells about the type of trends (increasing or decreasing), which is clearly indicated by the KRC and MK tests.Pingale*et al.* (2015) also reported the similarity in results of annual rainfall trendsdetected by the MK test, MK test with pre-whitening and modified MK test.Therefore, in this study, results of the KRC and MK tests are preferred over the SROC test.

3.3.2 Seasonal Rainfall

Spatial trends of the seasonal rainfall for four seasons, i.e. pre-monsoon, monsoon, post-monsoon, and non-monsoon, are depicted in Figure 6. It is seen from the results of the SROC test that the trends in the pre-monsoon season are statistically-significant only in 36464.5 km^2(19.6%) area, which mainly exist in the southern portion (Figure 6a). The trends are highly-significant in six districts including Navsari and Valsad at 0.01 l.s. (Table 2). Both the KRC and MK tests showed decreasing trends in 74.4 and 75% area, respectively in the pre-monsoon season, with statistically-significant trends in 16009 (8.6%) and 14455.4 (7.8%) km^2, respectivelyat 0.10 l.s. In contrast, increasing trends are distributed over 47560.6 (25.6%) and 46473.2 (25%) $km^2$by the KRC and MK tests, respectively, which are almost non-significant in the entire area. The significantly increasing trends are detected in some pockets of 3 districts (Kachchh, Bhavnagar and Bharuch) by both the KRC and MK tests (Figure 6b,c). On the contrary, the statistically-significant decreasingtrends are revealed in four districts, i.e. Valsad (0.05 l.s.), Porbandar (0.05 l.s.), The Dang (0.10 l.s.), and Navasari (0.01 l.s.) from the KRC test (Table 3).The MK testalso showedstatistically-significant decreasing trends in Navsari, The Dang and Valsad districts at 0.05 l.s. (Table 4). It is clearly observed from the above discussion that the results of the KRC and MK tests are almost similar to each other for pre-monsoon rainfall.

In monsoon season, the SROC test identified the statistically-significant trends in 140074.1 km^2 (75.3%) at 0.10 l.s. spreading all over the area except in the southern portion (Figure 6d). The KRC test indicated the significant trends over 39452.8 (21.2%) and 95463.4 km^2 (51.3%) at l.s. of 0.05 and 0.10, respectively (Figure 6e), whereas, the MK test showed the significant trends over 27481.4(14.8%) and 71379.6km^2 (38.4%) at the same l.s., respectively. The highly-significant increasing trends at 0.05 and 0.01 l.s. are concentrated over the northwest region of

Kachchh, pockets of Saurashtra and northeast regions of the area. It can be seen from Tables 3 and 4 that the significantly increasing trends in the monsoon rainfall at 0.10 l.s. exist in 11 and 5districts from the KRC and MK tests, respectively, whereas the SROC test showed significant trends in 15 districts (Table 2) at the same l.s. The decreasing trends of the monsoon rainfall are located in the southern portion, which are not statistically-significant at anyl.s. The monsoon trends are very similar to annual trends except some portions of western Kachchh and Patan districts, which is consistent withfindings of Pingale*et al.*(2014).

In the post-monsoon season, the significant trends are not found in a large (92.9%) area by the SROC test (Figure 6g). Almostsimilar results, obtained bythe KRC and MK test, further illustrated that the decreasing trends are prevailing over large areas, i.e.152974.8 (82.3%) and 153682.5 (82.7%) km^2,respectively in comparison to areaunderthe increasing trends, i.e.32936.6 (17.7%) and 32228.9 (17.3%) km^2,respectively (Figures6h,i). Very less area of 68 (0.04%) $km^2$is found to have statistically-significant increasing trends at 0.10 l.s. byKRC and MK tests;however, the significantly-decreasing trends at 0.10 l.s. are seen over the small areas. At district level, none ofthe tests revealed statistically-significant trend (Tables 2, 3, and 4).

Results of the three trend tests for the non-monsoon season'srainfall, are more or less similar to each other (Figures6j,k,l). The SROC test revealed the significant trends in 73468.4 km^2 (39.5%) at 0.10 l.s., mostly spreading in the middle and southwest portions (Figure 6j). Whereas, the KRC and MK tests obtained the decreasing trends in 173559.9 (93.4%) km^2, compared to 12351.5 (6.6%) km^2having the increasing trends. Of the total areas showing the decreasing trends, the results of the KRC and MK tests showed that 41357.1 (22.2%) and 42763.7 (23%) km^2 area, respectively have the statistically-significant trends at 0.10 l.s. Only seven and five, of the total 26 districts, showed a significant decrease in the non-monsoon rainfall at 0.10 l.s. from the KRC and MK tests, respectively; the trends in other districts were having the non-significantly decreasing rainfall (Tables 3and 4).

3.3.3 Monthly and One-Day Maximum Rainfall

Results of three trend tests depicting the spatial trends of the monthly maximum and one-day maximum rainfall are presented in Figure 7. It is seen from Figure 7a that the significant trends of the monthly maximum rainfall are present over125024.3 km^2 (67.2%) as revealed from the SROC test. The results of both the KRC and MK tests (Figures7b, c), however, found the increasing trends over177141.6 (95.3%) km^2 area. The decreasing trends were present in relatively less area, i.e. 8769.8 (4.7%) km^2 from both the KRC and MK tests. The significantly-increasing trends at 0.10 l.s. from the KRC and MK tests are found in 77672.4 (41.8%) and 43640.9 (23.5%) km^2 area respectively, which areprevalent in the middle and northeast portions. The district-level analysis indicated that more than 60% area (including 16 districts) showed a significant trend (Figure 7a) ofthe monthly maximum rainfall from the SROC test, and of that, the highly-significant trends are observed in 11 districts (Ahmadabad, Amreli, Anand, Banaskantha, Bhavnagar, Dahod, PanchMahals, Patan, Rajkot, Sabarkantha

and Surendranagar) at 0.05 l.s. (Table 2) and in Mahesanadistrict (0.01 l.s.). The KRC test revealed the significantly-increasing trends at 0.05 l.s. in Mehsana and Sabarkantha districts, whereas, the MK test found a significant increase in the monthly maximum rainfall at 0.05 l.s. intwo districts, i.e. Dahod andSabarkantha(Tables 3 and 4). The results of the KRC and MK tests closely matched to each other, and slightly deviated from the results of the SROC tests.

In case of the one-day maximum rainfall, it is observed from the results of the SROC tests presented in Figure 7d that the significant rainfall trends are distributed over the small areas extending over 45744.1 km^2 (24.6%). Results of both the KRC and MK tests showed the increasing trends in comparatively large areas (139036 km^2, 74.8%) than that underthe decreasing trends (46875.4 km^2, 25.2%). However, the increasing trends are found statistically-significant at 0.10 l.s. only in 16884.5 (9.1%) and 14744.5 (7.9%) km^2 areas, from the KRC and MK tests, respectively. On the other hand, all the decreasing trends are found non-significant at all l.s. excluding very small area of 2441 km^2 (1.3%), which showed statistically-significant decreasing trend at 0.10 l.s. At district-level, the significant trends in one-day maximum rainfall could be obtained in three districts, i.e. Amreli, Tapi and The Dang from the SROC test (Table 2). Whereas, the KRC test found the significantly-decreasing trends in The Dang district only (Table 3) at 0.10 l.s. andthe MK test did not findany significant trend. The assessment of trends of extreme annual daily rainfall events is crucial for adaptationplanning in arid regions of India (Pingale*et al.*2014).

3.4Comparisons of Spatially-DistributedTrends

Results of three trend tests are spatially compared through union analysis for five possible combinations of similar and dissimilar trends, and the results of the same for all seven types of rainfall raster datasets are presented in Figure 8. It is seen from Figure 8(a that in case of annual rainfall, the results of the KRC and MK tests are in good agreement in 104690.6 km^2 (56.3%) area whereas, results of all the tests are found in good coherence in 57840.8 km^2 (31.1%) area. In contrast, results of all the tests showed strong harmony to each other in majority of the area when applied to pre-monsoon (156897.2 km^2, 84.4%) and post-monsoon (171350.6 km^2, 92.2%) seasons (Figures8b,d). In both the rainfalls, the second dominating combination is for the similar results obtained from the KRC and MK tests. Similarly, for the monsoon season, the results of the KRC and MK tests revealed spatial consistency to each other in 91887.5 km^2 (49.4%) area, and results of all tests are close to each other in 69581.5 km^2 (37.4%) area (Figure 8c). In non-monsoon season, similar results of all the tests are found in 126127.4 km^2 (67.8%) area, whereas the similar results from the KRC and MK tests are obtained in 41793.8 km^2 (22.5%) area (Figure 8e). The results of the KRC and MK tests for monthly maximum rainfall were observed to be the similar in 76295 km^2 (41%) area with dominancy of the similar results of all the tests in 73563.5 km^2 (39.6%) area (Figure 8f). Finally, the results of the trend tests applied to one-day maximum rainfall depicted similarity of all three tests' results in amajor portion, i.e. 146678 km^2 (78.9%), whereas, the similar spatial trends were obtained from the KRC and MK tests' results in 36370.2 km^2 (19.6%)

area.The good harmony in the results of KRC and MK tests is also reported in earlier studies dealing with rainfall trend analysis, e.g. Machiwal and Jha 2008, Machiwal*et al.* 2016, Machiwal and Jha 2016.

Based on the above discussion, it is clearly observed that of the total possible five situations of the test results, two combinations, i.e. SROC-KRC-MK (similar results of all three tests) and KRC-MK (close agreement of the KRC and MK tests) predominantly exist in all the seven types of rainfall datasets. Also, it is seen that the trends identified in the pre-monsoon, post-monsoon and one-day maximum rainfalls by three trends tests are consistent in a major portion with the largest agreement in more than 92% area for the post-monsoon rainfall. The dissimilar results of all three trend tests were obtained maximum (13.7% area)in case of -monthly maximum and minimum (0.38% area) for post-monsoon rainfall series.

From the earlier discussion of trend results of seven types of rainfall series, it is inferred that significantly-increasing trends are the most-prominent in rainfall series of large magnitudes, i.e. annual, monsoon and monthly-maximum. These increasing rainfall trends are dominantly seen in the northeast, southwest and northwest portions of the area.On the contrary, decreasing rainfall trends are depicted in the low-magnitude rainfall series ofpre-monsoon, post-monsoon and non-monsoon seasons. However, decreasing trends are significant only in pre-monsoon (mainly in southeast portion) and non-monsoon (in northeast and southwest portions) seasons. Furthermore, it is interesting to notice that the southeast portion shows a different behavior from the rest of the area in case of annual, pre-monsoon, monsoon, and monthly-maximum rainfall.It is revealed that the decreasing rainfall trends are prevailing in the southeast portion where the rainfall magnitudes generally remains higher than the rest of the area.

4. CONCLUSIONS

This study employed the rainfall datasets collected from the satellite-sensors, i.e. Tropical Rainfall Measurement Mission (TRMM) at high resolution of 0.25º×0.25º for spatial modelling of the rainfall trends. The novelty of the study lies in developing a standard methodology for identifying the trends in the raster datasets by exploring capabilities of the geographical information system (GIS) in implementing procedures of the three trend detection tests, i.e. Spearman rank order correlation (SROC), The Kendall's rank correlation (KRC) and Mann-Kendall (MK) tests. The developed methodology is demonstrated by applying it to TRMM rainfall raster datasets of the Gujarat State of India.

The mean annual rainfall in the study area varied from less than 400 mm to more than 1500 mm with the SD of less than 200 mm to more than 350 mm. The coefficient of variation indicated the large variability of the annual rainfall in the areas experiencing relatively scanty rainfall. The results of the KRC and MK tests showed a very high degree of coherence in spatial distribution of the identified trends for all seven types of the rainfall datasets. The significantly increasing rainfall trends in the annual (39.9% area), monsoon season (38.4%

area), and monthly-maximum (23.5% area) rainfall are found to be prevalent in the Saurashtra-Kachchh region situated in the northwest and southwest portions, and in a fringe located in the northeast portion. On the contrary, the negative trends of the annual rainfall are mainly confined within the southeast portion of the area but none of them could be found as the statistically-significant. In the pre-monsoon season, the significantly decreasing rainfall trends are indicated in the southeast portion whereas both the increasing and decreasing rainfall trends are not statistically-significant in the post-monsoon season except in some negligible scattered patches. In the non-monsoon season, significantly-decreasing rainfall trends (23% area) are observed in the Saurashtra region and middle portion of the area. In one-day maximum rainfall, increasing trends are quite significant (7.9% area) in the middle of Saurashtra region, few patches of the northeast portion, and some area in Kachchh region,andmajor portion of the area (65.7%) depicted non-significant increasing trends.

Comparative evaluation of the three trend tests revealed that their results were in fair agreement with each other in a major portion of the area for the pre-monsoon, post-monsoon, non-monsoon and one-day maximum rainfall. On the other hand, the spatial distribution of the trends identified by the KRC and MK tests was found to be the exactly similar in a large proportion of the area for the annual (56.3%), monsoon (49.4%) and monthly maximum (41%) rainfall. This finding suggests robustness of the KRC and MK tests in detecting the trends in the hydrologic time series. Moreover, the methodology developed in this study can be easily employed in other parts of the world to examine rainfall trends and to model their spatial variability by utilizing satellite-based raster datasets at very high resolution.

ACKNOWLEDGEMENTS

Authors are grateful to twoanonymous reviewers and the editor for their valuable comments and useful suggestions,which helped improving earlier version of this article.

REFRENCES

Asadieh, B. and Krakauer, N.Y., 2015.Global trends in extreme precipitation:climate models versus observations. Hydrology and Earth System Sciences, 19, 877-891

Bal, P.K., Ramachandran, A., Geetha, R., Bhaskaran, B., Thirumurugan, P., Indumathi, J. and Jayanthi, N., 2016. Climate change projections for Tamil Nadu, India: derivinghigh-resolution climate data by a downscaling approach usingPRECIS. Theoretical and Applied Climatology, 123 (3), 523-535

CRU, 2000.Climate Research Unit, University of East Anglia. http://www.cru.uea.ac.uk. accessedon 10-May 2016

Das, P.K., Chakraborty, A. and Seshasai, M.V.R., 2014. Spatial analysis of temporal trend of rainfall and rainy days duringthe Indian Summer Monsoon season using daily gridded (0.5° × 0.5°)rainfall data for the period of 1971–2005. Meteorological Applications, 21, 481-493.

Diem, J.E., Ryan, S.J., Hartter, J. and Palace, M.W., 2014. Satellite-based rainfall data reveal a recent drying trend in central equatorial Africa. Climatic Change, 126, 263-272

Gokmen, M., Vekerdy, Z., Verhoef, W. and Batelaan, O., 2013.Satellite-based analysis of recent trends in the ecohydrology of a semi-arid region.Hydrology and Earth System Sciences, 17, 3779-3794

Goswami, B.N., Venugopal, V., Sengupta, D., Madhusoodanan, M.S. and Xavier, P.K., 2006. Increasing trend of extreme rain events over India in a warming environment, Science, 314, 1442–1444

Goyal, M.K., 2014. Statistical analysis of long term trends of rainfall during 1901-2002 at Assam, India. Water Resources Management, 28, 1501-1515

GSFC, 2015.Readme Document for the Tropical Rainfall Measurement Mission.Earth Sciences Data and Information Services Center (GESDISC). NASA Goddard Space Flight Center, Code 610.2, Greenbelt, MD 20771 USA

Guhathakurta, P., Sreejith, O.P. and Menon, P.A., 2011. Impact of climate change on extreme rainfall events and flood risk in India. Journal of Earth System Science, 120(3), 359-373

Hamed, K.H., 2008. Trend detection in hydrologic data: TheMann–Kendall trend test under the scaling hypothesis. Journal of Hydrology, 349, 350-363

Hoscilo, A., Balzter, H., Bartholomé, E., Boschetti, M., Brivio, P.A., Brink, A., Clerici, M. and Pekel, J.F., 2015. A conceptual model for assessing rainfall and vegetationtrends in sub-Saharan Africa from satellite data.International Journal of Climatology, 35, 3582-3592

Huffman, G.J., Adler, R.F., Bolvin, D.T., Nelkin, E.J., Kenneth, P.B., 2007. The TRMM multi-satellite analysis (TMPA): quasi-global, multiyear, combined-sensor precipitation estimates at fine scales. Journal of Hydrometeorology, 8, 38–55

Huffman, G.J., Adler, R.F., Rudolf, B., Schneider, U. and Kenneth, P.B., 1995. Global precipitation estimates based on a technique for combining satellite-based estimates, rain gauge analysis, and NWP model precipitation information. Journal of Climate, 8, 1284–1295

Jain, S.K. and Kumar, V., 2012. Trend analysis of rainfall and temperature data for India. Current Science, 102(1), 37-49

Jayawardena, A.W. and Lai, F., 1989.Time series analysis of water quality data in Pearl river, China. Journal of Environmental Engineering, ASCE, 115(3), 590-607

Joshi, M.K. and Pandey, A.C., 2011. Trend and spectral analysis of rainfall over Indiaduring 1901–2000. Journal of Geophysical Research, 116, D06104, DOI: 10.1029/2010JD014966

Joyce, R.J., Janowiak, J.E., Arkin, P.A., Xie, P., 2004. CMORPH: a method that produces global precipitation estimates from passive microwave and infrared data at high spatial and temporal resolution. Journal of Hydrometeorology, 5, 487–503

Kanamitsu, M., Ebisuzaki, W., Woollen, J., Yang, S.K., Hnilo, J.J., Fiorino, M. and Potter, G.L., 2002.NCEP-DOE AMIP-IIreanalysis (R-2). Bulletin ofthe American Meteorological Society, 83(11),1631–1643

Kendall, M.G., 1973. Time Series. Charles Griffin and Co. Ltd. London, U.K

Koutsoyiannis, D. and Montanari, A., 2007. Statistical analysis of hydroclimatic time series: Uncertainty and insights, Water Resources Research, 43, W05429, DOI:10.1029/2006WR005592

Krishnamurthy, C.K.B., Lall, U. and Kwon, H.-H., 2009.Changing frequency and intensity of rainfall extremes over India from 1951 to 2003. Journal of Climate, 22 (18), 4737-4746

Kumar, V., 2003. Rainfall characteristics of Shimla district (H.P.). Journal of Indian Water Resource Society, 23(1),1-10

Kumar, V. and Jain, S.K., 2010. Trends in rainfall amount and number of rainy days in river basins of India (1951-2004). Hydrology Research, 42(4), 290-306

Kumar, V., Jain S.K. and Singh Y., 2010. Analysis of long-term rainfall trends in India. Hydrological Sciences Journal, 55(4), 484-496

Kumar, V. ,Samtani, B.K. , Yadav, S.M. and Naresh, K., 2014. Decadal Comparison of Rainfall Seasonality Index in Gujarat.Global Sustainability Transitions: Impacts and Innovations. Edited by Mishra G.C. Excellent Publishing House, New Delhi, ISBN: 978-93-83083-77-0,238-245

Koutsoyiannis, D. and Montanari, A., 2007. Statistical analysis of hydroclimatic time series:Uncertainty and insights. Water Resources Research, 43, W05429, DOI:10.1029/2006WR005592

Lettenmaier, D.P., 1976. Detection of trends in water quality data from records with dependent observations. Water Resources Research, 12 (5), 1037-1046

Li, L., Xu, C.-Y., Zhang, Z. and Jain, S.K., 2014.Validation of a new meteorological forcing data in analysis of spatial and temporal variability of precipitation in India. Stochastic Environmental Research and Risk Assessment, 28 (2), 239-252

Liu, Q., Yang, Z. and Cui, B., 2008. Spatial and temporal variability of annual precipitation during 1961–2006 in Yellow River Basin, China. Journal of Hydrology, 361, 330-338

Machiwal, D. andJha, M.K., 2012. Hydrologic Time Series Analysis: Theory and Practice. Springer, Germany and Capital Publishing Company, New Delhi, India, 303p.

Machiwal, D. and Jha, M.K., 2008. Comparative evaluation of statistical tests for time series analysis: application to hydrological time series. Hydrological Sciences Journal, 53(2), 353-366

Machiwal, D. and Jha, M.K., 2016. Evaluating persistence, and identifying trends and abrupt changes in monthly and annual rainfalls of a semi-arid region in western India. Theoretical and Applied Climatology, DOI 10.1007/s00704-016-1734-9

Machiwal, D., Kumar, S. and Dayal, D., 2016.Characterizing rainfall of hot arid region by using time-series modeling and sustainability approaches: a case study from Gujarat, India. Theoretical and Applied Climatology, 124, 593-607

Manzanas, R., Amekudzi, L.K., Preko, K., Herrera, S. and Gutiérrez, J.M., 2014. Precipitation variability and trends in Ghana: An intercomparison of observational and reanalysis products. Climatic Change, 124 (4), 805-819

Matalas, N.C. and Langbein, W.B., 1962.Information content of the mean. Journal of Geophysical Research, 67(9), 3441-3448

McGhee, J.W., 1985. Introductory Statistics. West Publishing Co. New York, USA

Oguntunde, P.G., Abiodun, B.J. and Lischeid, G., 2011. Rainfall trends in Nigeria, 1901–2000. Journal of Hydrology, 411, 207-218.

Oza, M. and Kishtawal, C.M., 2014.Spatial analysis of Indian summer monsoon rainfall. Journal of Geomatics,8(1), 40-47

Pingale, S., Adamowski, J., Jat, M. and Khare, D., 2015.Implications of spatial scale on climate change assessments. Journal of Water and Land Development, 26, 37–56.

Pingale, S., Khare, D., Jat, M. and Adamowski, J., 2014.Spatial and temporal trends of mean and extreme rainfall and temperature for the 33 urban centers of the arid and semi-arid state of Rajasthan, India.Atmospheric Research 138, 73-90

Pombo, S. and de Oliveira, R.P., 2015. Evaluation of extreme precipitation estimates from TRMM in Angola. Journal of Hydrology, 523, 663-679

Qin, N.X., Chen, X., Fu, G.B., Zhai, J.Q. andXue, X.W., 2010. Precipitation and temperature trends for the Southwest China: 1960–2007. Hydrological Processes, 24(25), 3733–3744

Rajeevan, M., Bhate, J. andJaswal, A.K., 2008. Analysis of variability and trends of extreme rainfall events over India using 104 years of gridded daily rainfall data. Geophysical Research Letters, 35, L18707.DOI:10.1029/2008GL035143

Rathore, L.S., Attri, S.D. and Jaswal, A.K., 2013. State Level Climate Change Trends in India. Meteorological Monograph No.ESSO/IMD/EMRC/02/2013. India Meteorological Department, Lodi Road, New Delhi- 3 (India)

Ray, K., Mohanty, M. and Chincholikar J.R., 2009.Climate variability over Gujarat India. ISPRS Archives XXXVIII-8/W3 Workshop Proceedings:Impact of Climate Change on Agriculture December 17-18, 2009. Downloaded from http://www.isprs.org/proceedings/XXXVIII/8-W3/

Sang, Y.-F., Wang, Z. and Liu, C., 2014.Comparison of the MK test and EMD method for trend identification in hydrological time series. Journal of Hydrology, 510, 293-298

Sarkar J., Chicholikar J.R. and Rathore L.S., 2015. Predicting future changes in temperature and precipitation in arid climate of Kutch, Gujarat: analyses based on LARS-WG model. Current Science, 109(11), 2084-2093

Schneider, U., Becker, A., Meyer-Christoff, M.Z., Rudolf, B., 2010.Global precipitation analysis products of GPCC.Global Precipitation Climatology Centre.Deutscher Wetterdients Offenbach. Germany, 1–12

Sonali, P. and Kumar, D.N., 2013. Review of trend detection methods and their application to detect temperature changes in India. Journal of Hydrology, 476, 212-227

Sorooshian, S., Hsu, K., Gao, X., Gupta, H.V., Imam, B. and Braithwaite, D., 2000. Evolution of the PERSIANN system satellite-based estimates of tropical rainfall. Bulletin of the American Meteorological Society, 81(9), 2035–2046

Tabari, H. and Talaee, P.H., 2011. Temporal variability of precipitation over Iran: 1966-2005. Journal of Hydrology, 396, 313-320

Taxak, A.K., Murumkar, A.R. and Arya, D.S., 2014. Long term spatial and temporal rainfall trends and homogeneity analysis in Wainganga basin, Central India. Weather and Climate Extremes, 4, 50–61

TRMM, 2015. http://mirador.gsfc.nasa.gov/cgi-bin/mirador/presentNavigation.pl?tree=project&project=TRMM&dataGroup=Gridded (Accessed on April 08, 2015)

vonStorch, H., 1995. Misuses of statistical analysis in climate research. In: von Storch, H., Navarra, A. (Editors), Analysis ofClimate Variability: Applications of Statistical Techniques.Springer-Verlag, Berlin, pp. 11–26.

Wagesho, N., Goel, N.K. and Jain, M.K., 2013. Temporal and spatial variability of annual and seasonal rainfall over Ethiopia. Hydrological Sciences Journal, 58 (2), 354-373

Weedon, G.P., Gomes, S., Viterbo, P., Shuttleworth, W., Blyth, E., Österle, H., Adam, J., Bellouin, N., Boucher, O. and Best, M., 2011. Creation of the WATCH forcing data and its use to assess global and regional reference crop evaporation over land during the twentieth century. Journal of Hydrometeorology, 12(5), 823-848

Westra, S., Alexander, L.V. and Zwiers, F.W., 2013.Global increasing trends in annual maximum daily precipitation. Journal of Climate, 26, 3904-3918

WMO, 1988.Analysing long time series of hydrological data with respect to climate variability. WCAP-3, WMO/TD No. 224, the World Meteorological Organisation (WMO), Geneva, Switzerland

Yu, P.S., Yang, T.C. and Wu, C.K., 2002.Impact of climate change on water resources in southern Taiwan. Journal of Hydrology, 260(1-4),161-175

Yue, S., Pilon, P., Phinney, B. and Cavadias, G., 2002.The influence of autocorrelation on the ability to detect trend in hydrological series. Hydrological Processes, 16, 1807-1829

Yue, S. and Wang, C.Y., 2002.Applicability of prewhitening to eliminate the influence of serial correlation on the Mann-Kendall test. Water Resources Research, 38(6),4-1 – 4-7. DOI: 10.1029/2001WR000861

Table 1: Statistical summary of district-wise annual rainfall (1998-2013)

S. No.	District	Mean Annual Rainfall (mm)	Standard Deviation (mm)	Coefficient of Variation (%)
1	Ahmedabad	875.56	349.77	0.40
2	Amreli	786.15	304.77	0.39
3	Anand	1037.48	414.92*	0.40
4	Banaskantha	673.04	235.71	0.35
5	Bharuch	1168.61	355.67	0.31
6	Bhavnagar	894.10	321.07	0.36
7	Dahod	929.27	267.09	0.29
8	Gandhinagar	881.57	326.63	0.37
9	Jamnagar	789.06	343.87	0.44
10	Junagadh	843.23	312.72	0.37
11	Kachchh	502.78#	229.18#	0.46*
12	Kheda	981.12	343.74	0.35
13	Mahesana	832.52	320.37	0.38
14	Narmada	1255.26	328.88	0.26
15	Navsari	1742.39	332.38	0.19
16	Panch Mahals	1035.28	291.89	0.28
17	Patan	726.98	311.42	0.43
18	Porbandar	851.35	320.00	0.38
19	Rajkot	802.22	318.01	0.40
20	Sabarkantha	816.15	259.58	0.32
21	Surat	1343.83	334.58	0.25
22	Surendranagar	799.62	329.98	0.41
23	Tapi	1245.74	292.33	0.23
24	The Dangs	1473.91	251.26	0.17#

25	Vadodara	1077.99	323.58	0.30
26	Valsad	1882.23*	338.33	0.18

*Maximum; #Minimum

Table 2: Spearman rank order correlation test-statistics for 26 districts of Gujarat

District	Annual	Pre-monsoon	Monsoon	Post-monsoon	Non-monsoon	Daily-maximum	Monthly-maximum
Ahmedabad	1.30	0.46	1.38*	1.11	1.51*	0.51	1.93#
Amreli	1.97#	0.37	1.97#	0.51	1.18	1.37*	2.09#
Anand	1.36*	0.77	1.25	0.77	1.95#	0.85	2.13#
Banaskantha	2.02#	0.23	2.31#	0.94	1.01	0.73	1.78#
Bharuch	1.14	1.38*	0.99	0.25	1.41*	0.84	1.22
Bhavnagar	1.68*	1.05	1.48*	0.35	0.95	1.13	2.15#
Dahod	1.85#	0.52	1.79#	0.31	0.99	0.94	1.98#
Gandhinagar	1.40*	0.86	1.23	0.87	1.42*	0.59	1.43*
Jamnagar	2.03#	1.00	1.75*	0.80	1.24	1.13	1.57*
Junagadh	1.46*	0.80	1.68*	0.83	1.28	1.08	1.30
Kachchh	1.93#	0.59	2.30#	0.60	0.66	0.87	1.39*
Kheda	1.50*	0.70	1.35*	0.82	1.49*	0.63	1.32
Mahesana	1.89#	0.90	2.18	0.98	1.49*	1.08	3.23*#
Narmada	1.24	1.26	1.06	0.33	1.09	0.67	0.93
Navsari	0.27	3.50*#	0.54	0.12	1.08	0.94	0.34
Panch Mahals	1.96#	0.96	1.65*	0.54	1.62*	1.13	1.87#
Patan	1.68*	0.49	2.03#	0.97	1.58*	0.89	1.95#
Porbandar	1.80#	2.02#	2.04#	0.86	1.58*	1.14	1.40*
Rajkot	1.93#	0.56	1.92#	0.82	1.49*	1.21	2.00#
Sabarkantha	2.15#	0.97	2.28#	1.09	1.30	1.28	2.55#
Surat	0.49	1.81#	0.59	0.24	1.10	1.00	0.59
Surendranagar	1.83#	0.40	1.64*	1.02	1.66*	0.66	2.31#
Tapi	0.33	1.22	0.28	0.53	1.33	1.40*	0.90
The Dangs	0.08	1.94#	0.28	0.43	1.25	1.98#	0.39

Vadodara	1.37*	1.08	1.15	0.48	1.53*	0.75	1.34
Valsad	0.29	2.81*#	0.42	0.20	0.73	0.51	0.37

*Trend at 0.10 l.s.; #Trend at 0.05 l.s.; *#Trend at 0.01 l.s.

Table 3: Kendall's rank correlation test-statistics for 26 districts of Gujarat

District	Annual	Pre-monsoon	Monsoon	Post-monsoon	Non-monsoon	Daily-maximum	Monthly-maximum
Ahmedabad	1.07	-0.43	1.17	-1.09	-1.65*	0.18	1.56
Amreli	1.88*	-0.24	1.81*	-0.87	-1.46	1.11	1.74*
Anand	1.15	-0.71	1.22	-0.81	-1.82*	0.71	1.76*
Banaskantha	1.72*	0.03	1.87*	-0.85	-1.16	0.60	1.48
Bharuch	0.96	-1.40	0.87	-0.36	-1.21	0.69	1.04
Bhavnagar	1.60	0.87	1.39	-0.05	-0.78	0.54	1.68*
Dahod	1.82*	-0.56	1.70*	-0.17	-1.08	0.85	1.86*
Gandhinagar	1.26	-0.82	1.19	-0.95	-1.80*	-0.49	1.07
Jamnagar	1.84*	-1.10	1.64*	-0.58	-1.18	0.96	1.42
Junagadh	1.61	-0.73	1.66*	-1.20	-1.53	0.88	1.35
Kachchh	1.69*	0.32	1.97#	-0.15	-0.40	0.71	1.16
Kheda	1.44	-0.60	1.38	-0.90	-1.49	0.43	1.07
Mahesana	1.60	-0.94	1.78*	-0.81	-1.84*	0.72	2.46#
Narmada	1.06	-1.30	0.82	-0.23	-0.97	0.16	0.89
Navsari	-0.59	-2.80*#	-0.82	0.05	-0.99	-0.74	-0.33
Panch Mahals	1.89*	-0.96	1.68*	-0.63	-1.47	1.07	1.81*
Patan	1.41	-0.22	1.59	-0.80	-1.67*	0.66	1.53
Porbandar	1.94*	-2.06#	1.98#	-1.26	-1.71*	1.15	1.44
Rajkot	1.83*	-0.50	1.77*	-0.84	-1.48	1.09	1.75*
Sabarkantha	1.92*	-0.91	1.93*	-0.93	-1.59	1.12	2.00#
Surat	-0.09	-1.57	-0.24	0.03	-1.01	-0.90	0.04
Surendranagar	1.68*	-0.36	1.48	-0.89	-1.72*	0.46	1.95*
Tapi	-0.27	-1.15	-0.74	-0.41	-1.22	-1.32	-0.99
The Dangs	-0.09	-1.81*	-0.16	-0.33	-1.14	-1.84*	0.14

Vadodara	1.20	-1.09	1.04	-0.42	-1.33	0.76	1.19
Valsad	-0.41	-2.36[#]	-0.69	0.18	-0.70	-0.35	0.10

[*]Trend at 0.10 l.s.; [#]Trend at 0.05 l.s.; [*#]Trend at 0.01 l.s.

Note: Negative and positive values denotes decreasing and increasing trends, respectively

Table 4: Mann-Kendall test-statistics for 26 districts of Gujarat

District	Annual	Pre-monsoon	Monsoon	Post-monsoon	Non-monsoon	One-day maximum	Monthly maximum
Ahmedabad	0.90	-0.40	0.84	-1.19	-1.72*	-0.12	1.12
Amreli	1.87*	-0.30	1.90*	-1.03	-1.56	1.28	0.91
Anand	0.53	-0.58	0.60	-1.13	-1.66*	0.63	1.09
Banaskantha	1.46	0.04	1.33	-0.85	-1.11	0.81	1.52
Bharuch	0.76	-0.68	0.77	-0.27	-0.92	0.45	0.94
Bhavnagar	1.38	0.37	1.17	-0.27	-1.14	0.37	0.97
Dahod	1.60	-0.42	1.48	-0.11	-1.15	0.93	1.96#
Gandhinagar	1.15	-0.44	0.89	-1.31	-1.85*	-0.06	1.73*
Jamnagar	1.91*	-0.39	1.72*	-0.09	-0.70	0.98	1.28
Junagadh	1.48	-0.96	1.57	-1.16	-1.42	0.45	1.03
Kachchh	1.61	0.27	1.97#	-0.14	-0.34	0.75	1.23
Kheda	0.97	-0.47	0.95	-1.07	-1.33	0.49	1.18
Mahesana	1.26	-0.67	1.11	-0.89	-1.79*	0.46	1.80*
Narmada	0.29	-1.01	-0.04	-0.29	-1.31	-0.70	-0.12
Navsari	-0.20	-2.08#	-0.48	0.02	-1.01	-0.30	-0.05
Panch Mahals	1.64*	-0.76	1.14	-0.71	-1.34	0.69	1.71*
Patan	1.12	0.12	1.12	-0.80	-1.22	0.73	1.39
Porbandar	1.79*	-1.22	1.91*	-0.83	-1.37	0.97	0.95
Rajkot	1.77*	-0.77	1.71*	-0.85	-1.48	1.10	1.16
Sabarkantha	1.67*	-0.92	1.48	-0.97	-1.73*	1.24	2.27#
Surat	-0.26	-1.47	-0.60	0.32	-0.89	-1.18	-0.21
Surendranagar	1.60	-0.42	1.49	-0.88	-1.61	0.65	1.48
Tapi	0.05	-1.47	-0.19	-0.37	-0.96	-0.99	-0.47
The Dangs	-0.14	-2.10#	-0.40	-0.26	-1.22	-1.44	0.18

Vadodara	1.12	-1.20	1.08	-0.51	-1.13	0.79	1.33
Valsad	-0.36	-2.12[#]	-0.69	0.17	-0.61	-0.47	0.12

[*]Trend at 0.10 l.s.; [#]Trend at 0.05 l.s.

Note: Negative and positive values denotes decreasing and increasing trends, respectively

Figure Captions

Figure 1. Location map of the study area showing districts of Gujarat State, India

Figure 2. Flowchart depicting step-by-step procedures for applying Spearman rank order correlation, Kendall rank correlation, and Mann-Kendall tests for identifying the trends in raster datasets

Figure 3. Spatial distribution of the (a) mean, (b) standard deviation, and (c) coefficient of variation of the annual rainfall for 16-year (1998-2013) period

Figure 4. Distribution of serial correlation at lag-1 for different time series

Figure 5. Spatial distribution of the annual rainfall trends identified at three level of significance (l.s.) by (a) Spearman Rank Order Correlation (SROC), (b) Kendall Rank Correlation (KRC), and (c) Mann-Kendall (MK) tests

Figure 6. Spatial distribution of the rainfall trends for pre-monsoon, monsoon, post-monsoon and non-monsoon seasons identified at three level of significance (l.s.) by Spearman Rank Order Correlation (SROC), Kendall Rank Correlation (KRC), and Mann-Kendall (MK) tests

Figure 7. Spatial distribution of the rainfall trends for monthly maximum and one-day maximum rainfalls identified at three level of significance (l.s.) by Spearman Rank Order Correlation (SROC), Kendall Rank Correlation (KRC), and Mann-Kendall (MK) tests

Figure 8. Distribution of similar and dissimilar results of the three trend tests in possible combinations over the study area

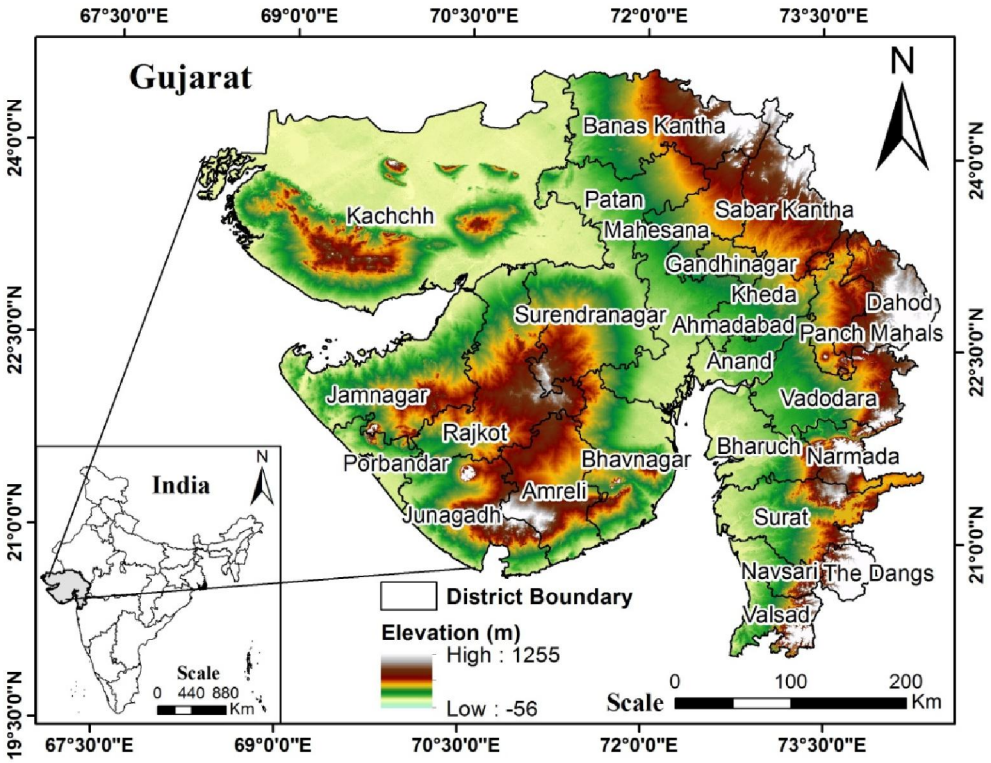
Gujarat
India
N
Banas Kantha
Patan
Sabar Kantha
Kachchh
Mahesana
Gandhinagar
Kheda
Dahod
Surendranagar
Ahmadabad
Panch Mahals
Anand
Jamnagar
Vadodara
Rajkot
Bharuch
Narmada
Porbandar
Bhavnagar
Amreli
Junagadh
Surat
Navsari
The Dangs
Valsad
District Boundary
Elevation (m)
High : 1255
Low : -56
Scale
0 440 880 Km
0 100 200 Km
67°30'0"E
69°0'0"E
70°30'0"E
72°0'0"E
73°30'0"E
24°0'0"N
22°30'0"N
21°0'0"N
19°30'0"N

Figure1

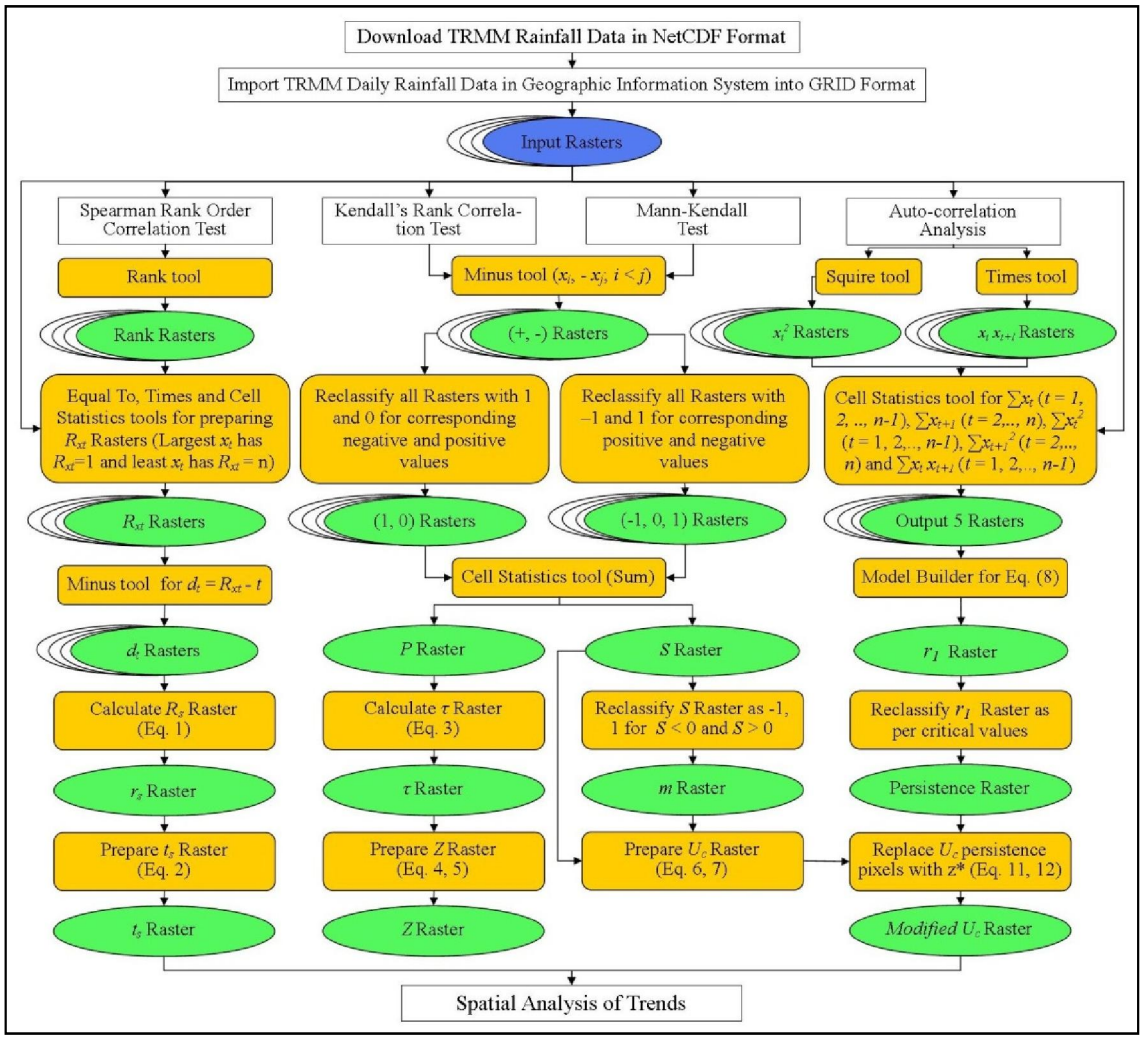
Download TRMM Rainfall Data in NetCDF Format
Import TRMM Daily Rainfall Data in Geographic Information System into GRID Format
Input Rasters
Spearman Rank Order Correlation Test
Kendall's Rank Correlation Test
Mann-Kendall Test
Auto-correlation Analysis
Rank tool
Minus tool (x_i, - x_j; $i < j$)
Squire tool
Times tool
Rank Rasters
(+, -) Rasters
x_i^2 Rasters
$x_i\, x_{i+l}$ Rasters
Equal To, Times and Cell Statistics tools for preparing R_{xt} Rasters (Largest x_t has R_{xt}=1 and least x_t has R_{xt} = n)
Reclassify all Rasters with 1 and 0 for corresponding negative and positive values
Reclassify all Rasters with –1 and 1 for corresponding positive and negative values
Cell Statistics tool for $\sum x_t$ (t = 1, 2, .., n-1), $\sum x_{t+l}$ (t = 2,.., n), $\sum x_t^2$ (t = 1, 2,.., n-1), $\sum x_{t+l}^2$ (t = 2,.., n) and $\sum x_t\, x_{t+l}$ (t = 1, 2,.., n-1)
R_{xt} Rasters
(1, 0) Rasters
(-1, 0, 1) Rasters
Output 5 Rasters
Minus tool for $d_t = R_{xt} - t$
Cell Statistics tool (Sum)
Model Builder for Eq. (8)
d_t Rasters
P Raster
S Raster
r_1 Raster
Calculate R_s Raster (Eq. 1)
Calculate τ Raster (Eq. 3)
Reclassify S Raster as -1, 1 for $S < 0$ and $S > 0$
Reclassify r_1 Raster as per critical values
r_s Raster
τ Raster
m Raster
Persistence Raster
Prepare t_s Raster (Eq. 2)
Prepare Z Raster (Eq. 4, 5)
Prepare U_c Raster (Eq. 6, 7)
Replace U_c persistence pixels with z* (Eq. 11, 12)
t_s Raster
Z Raster
Modified U_c Raster
Spatial Analysis of Trends

Figure2

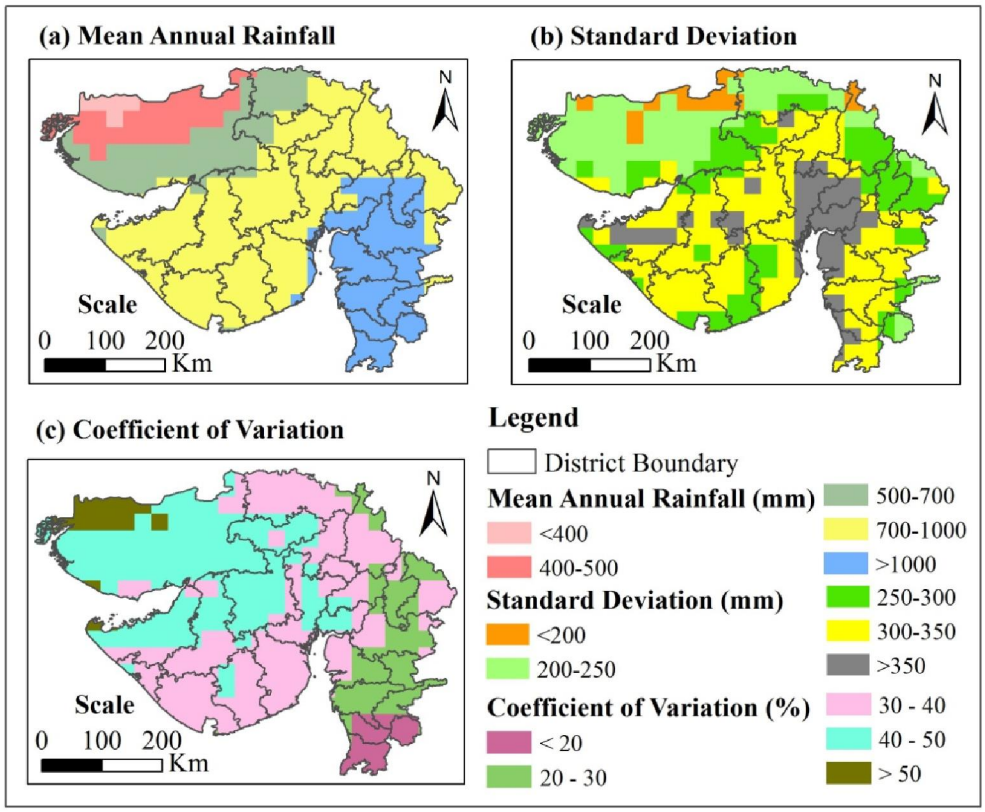
(a) Mean Annual Rainfall
N
Scale
0 100 200
Km
(b) Standard Deviation
N
Scale
0 100 200
Km
(c) Coefficient of Variation
N
Scale
0 100 200
Km
Legend
District Boundary
Mean Annual Rainfall (mm)
<400
400-500
500-700
700-1000
>1000
Standard Deviation (mm)
<200
200-250
250-300
300-350
>350
Coefficient of Variation (%)
< 20
20 - 30
30 - 40
40 - 50
> 50

Figure 3

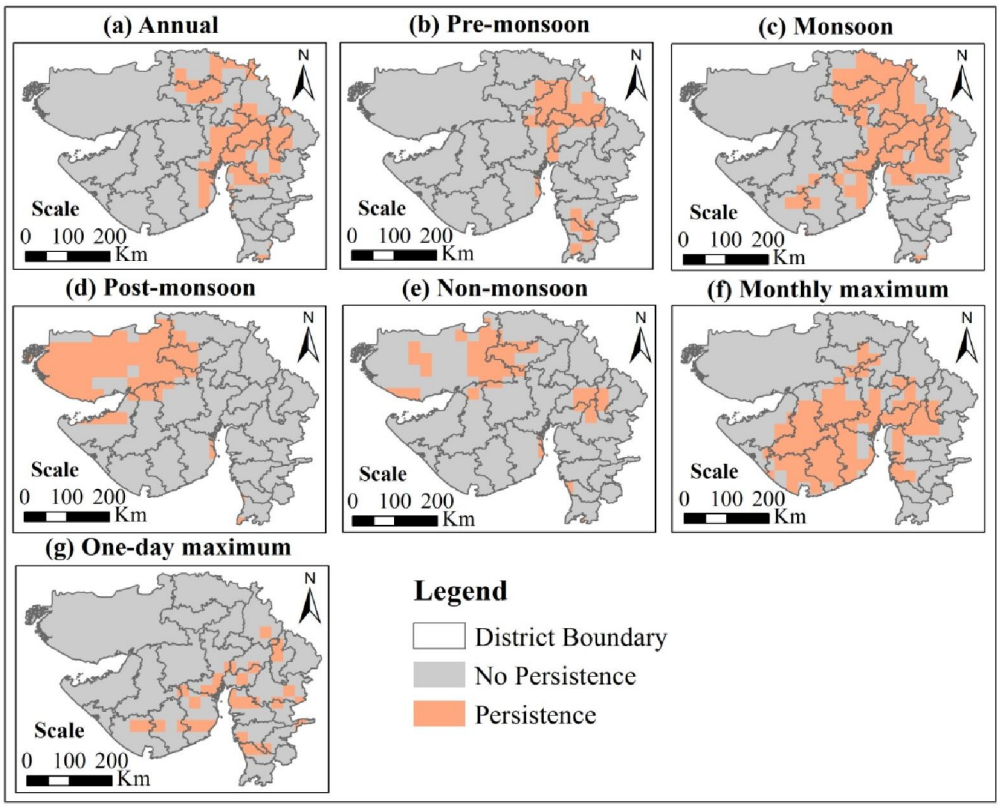
(a) Annual
(b) Pre-monsoon
(c) Monsoon
(d) Post-monsoon
(e) Non-monsoon
(f) Monthly maximum
(g) One-day maximum
N
Scale
0 100 200
Km
Legend
District Boundary
No Persistence
Persistence

Figure 4

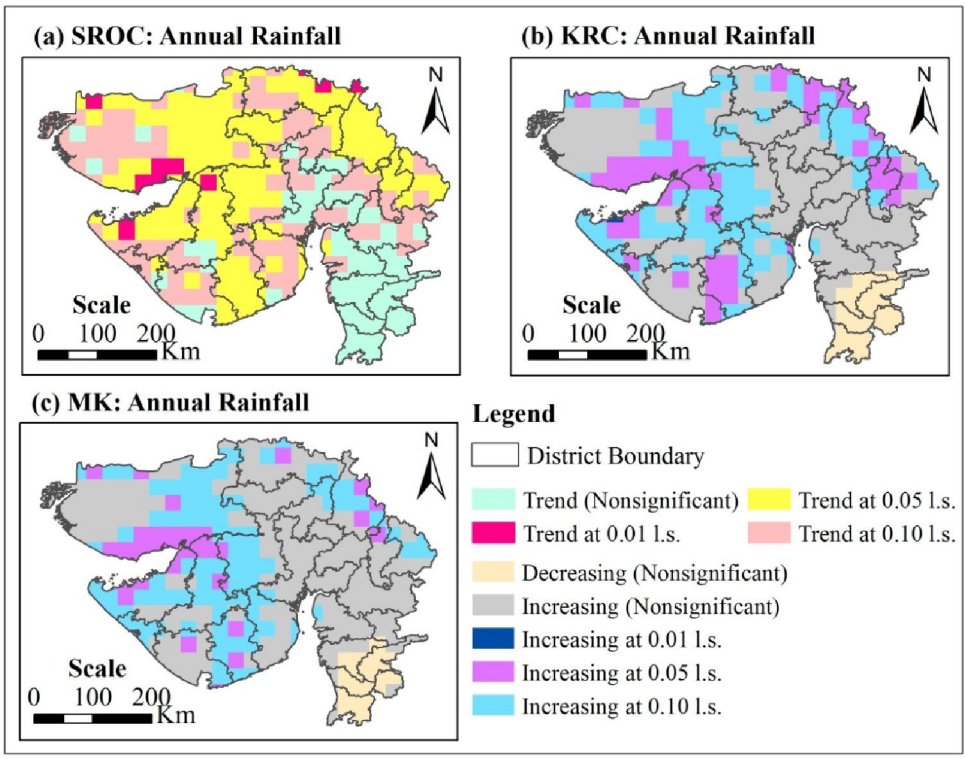
(a) SROC: Annual Rainfall
N
Scale
0 100 200
Km
(b) KRC: Annual Rainfall
N
Scale
0 100 200
Km
(c) MK: Annual Rainfall
N
Scale
0 100 200
Km
Legend
District Boundary
Trend (Nonsignificant)
Trend at 0.05 l.s.
Trend at 0.01 l.s.
Trend at 0.10 l.s.
Decreasing (Nonsignificant)
Increasing (Nonsignificant)
Increasing at 0.01 l.s.
Increasing at 0.05 l.s.
Increasing at 0.10 l.s.

Figure 5

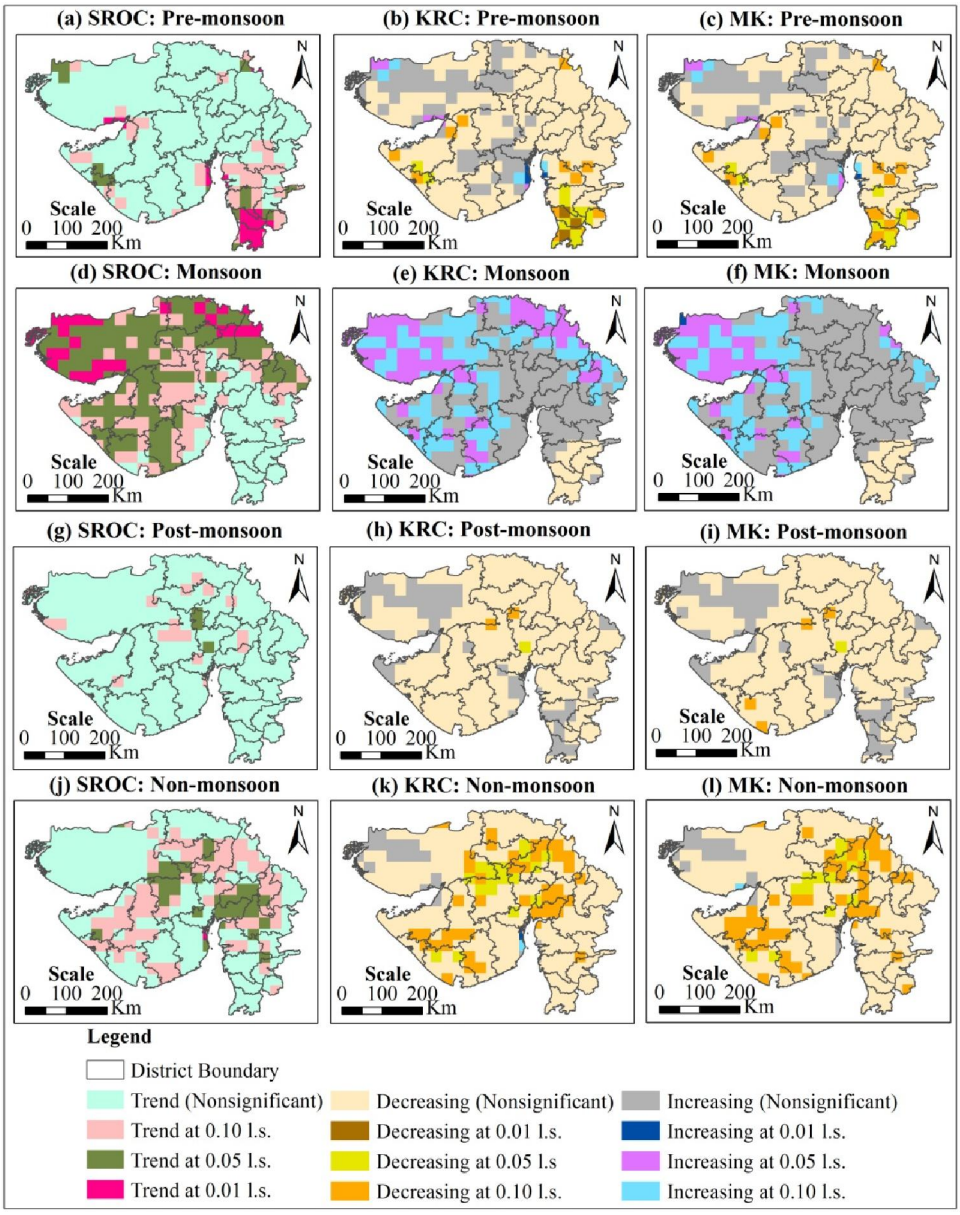
(a) SROC: Pre-monsoon
(b) KRC: Pre-monsoon
(c) MK: Pre-monsoon
(d) SROC: Monsoon
(e) KRC: Monsoon
(f) MK: Monsoon
(g) SROC: Post-monsoon
(h) KRC: Post-monsoon
(i) MK: Post-monsoon
(j) SROC: Non-monsoon
(k) KRC: Non-monsoon
(l) MK: Non-monsoon
N
Scale
0 100 200
Km
Legend
District Boundary
Trend (Nonsignificant)
Trend at 0.10 l.s.
Trend at 0.05 l.s.
Trend at 0.01 l.s.
Decreasing (Nonsignificant)
Decreasing at 0.01 l.s.
Decreasing at 0.05 l.s
Decreasing at 0.10 l.s.
Increasing (Nonsignificant)
Increasing at 0.01 l.s.
Increasing at 0.05 l.s.
Increasing at 0.10 l.s.

Figure 6

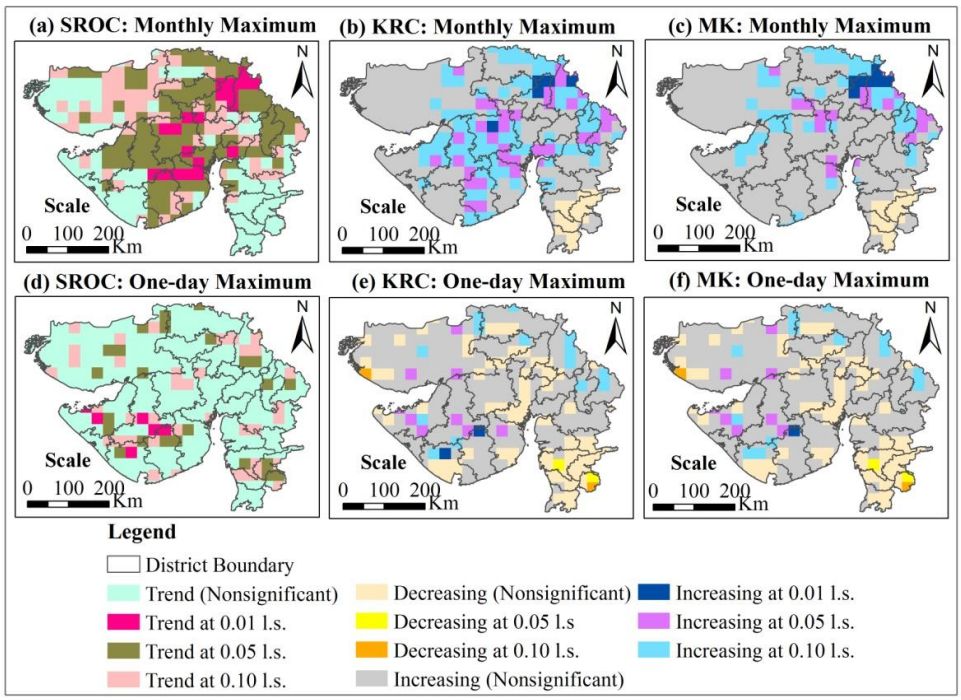
(a) SROC: Monthly Maximum
(b) KRC: Monthly Maximum
(c) MK: Monthly Maximum
(d) SROC: One-day Maximum
(e) KRC: One-day Maximum
(f) MK: One-day Maximum
N
Scale
0 100 200
Km
Legend
District Boundary
Trend (Nonsignificant)
Trend at 0.01 l.s.
Trend at 0.05 l.s.
Trend at 0.10 l.s.
Decreasing (Nonsignificant)
Decreasing at 0.05 l.s
Decreasing at 0.10 l.s.
Increasing (Nonsignificant)
Increasing at 0.01 l.s.
Increasing at 0.05 l.s.
Increasing at 0.10 l.s.

Figure 7

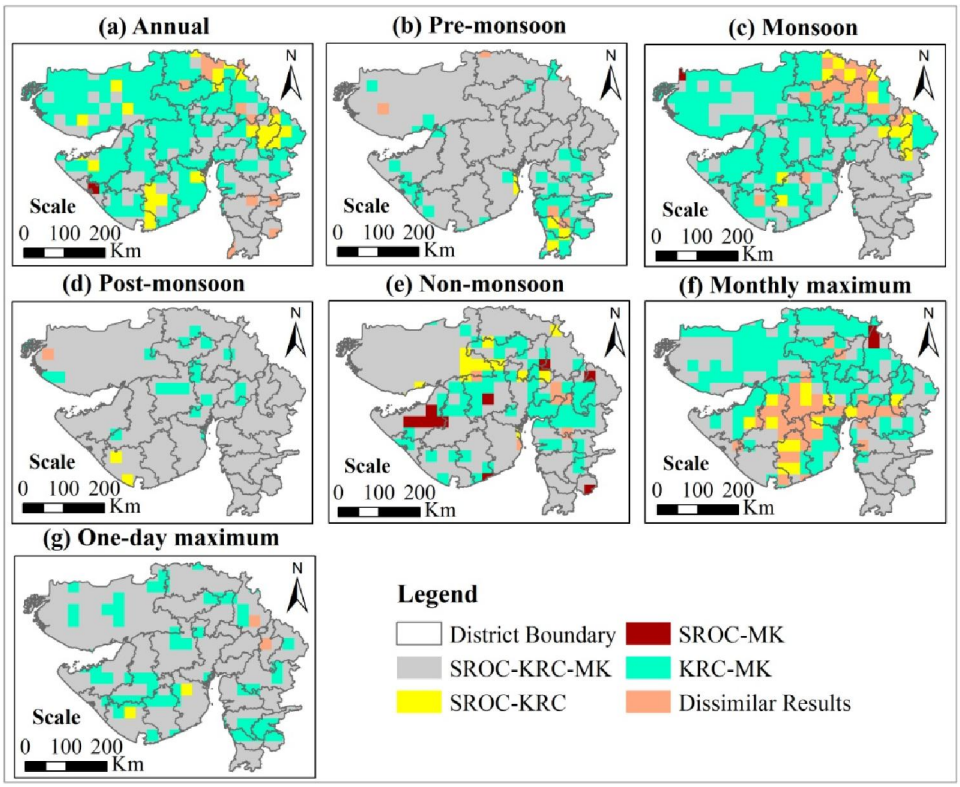
(a) Annual
(b) Pre-monsoon
(c) Monsoon
(d) Post-monsoon
(e) Non-monsoon
(f) Monthly maximum
(g) One-day maximum
N
Scale
0 100 200
Km
Legend
District Boundary
SROC-MK
SROC-KRC-MK
KRC-MK
SROC-KRC
Dissimilar Results

Figure 8